

# Direction-of-arrival estimation of a gravitational wave by correlations between quadrupole moments of pulsar timings

Taichi Ueyama<sup>a</sup> Hodaka Tamura<sup>a</sup> Hideki Asada<sup>a</sup>

<sup>a</sup>Graduate School of Science and Technology, Hirosaki University, Hirosaki 036-8561, Japan

E-mail: [h24ms103@hirosaki-u.ac.jp](mailto:h24ms103@hirosaki-u.ac.jp), [h25ms122@hirosaki-u.ac.jp](mailto:h25ms122@hirosaki-u.ac.jp),  
[asada@hirosaki-u.ac.jp](mailto:asada@hirosaki-u.ac.jp)

**Abstract.** Can we estimate the direction of arrival (DOA) of a gravitational wave (GW) signal from pulsar timing array observations? The present paper addresses the inverse problem, for which we consider quadrupole moments of pulsar timings due to GWs from a dominant isolated source such as a binary of supermassive black holes over an isotropic stochastic background. Correlations between the quadrupole moments are discussed, where the correlations between pulsar pairs over the full sky are taken into account. The correlations turn out to be in the form of a three-dimensional traceless matrix with rank 2 that can be closely related with a projection tensor for the GW. Thereby, we demonstrate that the rank-2 matrix allows to estimate the DOA of the GW. In expectation of the forthcoming Square Kilometer Array, angular resolutions as well as DOA estimation errors are also examined.

**Keywords:** gravitational waves / theory

**ArXiv ePrint:** [2602....](https://arxiv.org/abs/2602.21607)

---

## Contents

|          |  |           |
|----------|--|-----------|
| <b>1</b> | <b>Introduction</b>  | <b>1</b>  |
| <b>2</b> | <b>Correlations of quadrupole tensors</b>                      | <b>2</b>  |
| 2.1      | Setup and notations  | 2         |
| 2.2      | Correlations of quadrupole moments of pulsar timings           | 3         |
| <b>3</b> | <b>From quadrupole-moment correlations to DOA estimations</b>  | <b>5</b>  |
| <b>4</b> | <b>Discreteness, noises and estimation errors</b>              | <b>6</b>  |
| 4.1      | From a continuous limit to a discrete distribution of pulsars  | 6         |
| 4.2      | Angular resolution limited by the number of pulsars            | 7         |
| 4.3      | Estimation error from a random noise                           | 9         |
| 4.4      | Single dominant source over an isotropic stochastic background | 13        |
| <b>5</b> | <b>Summary</b>   | <b>13</b> |
| <b>A</b> | <b>Derivation of Eq. (2.12) with <math>C_A</math></b>          | <b>14</b> |
| <b>B</b> | <b>Relationship between quadratic polarization tensors</b>     | <b>16</b> |

---

## 1 Introduction

The idea of a search for gravitational waves (GWs) by using radio pulse timings can be dated back to Reference [1–3]. In their pioneering work, Hellings and Downs (HD) found that the sky correlation pattern of pulse timings among pulsar pairs depends upon the angle  $\gamma$  between the lines of sight to the pulsars viewed from Earth, and the correlation pattern can be a strong evidence of GWs [4], because it reflects the quadrupole nature of GWs [5–8]. See also Reference [9, 10] for a review on detection methods of stochastic GW backgrounds.

Eventually, several teams of pulsar timing arrays (PTAs) have reported a strong evidence of nano-hertz GWs [11–14]. According to these papers, a superposition of supermassive black hole binaries (SMBHBs) are among possible GW sources for the nano-hertz GWs, though improved methods, other possible explanations, and new physics searches have been widely argued e.g. [15–27]. A possible variance around the HD correlation as the mean has been discussed [28, 29].

If a single SMBHB dominates in a certain frequency bin for PTA observations, can we estimate the direction of arrival (DOA) for the GW? Currently, this issue is theoretical. See e.g. [30, 31] for methods for a single GW source detection by using PTAs.

Yet, it is expected that the near future Square Kilometer Array (SKA) will drastically increase the number of pulsars that can be used to significantly improve the sensitivity of PTAs. Sasaki et al. have recently proposed the use of a hemisphere in stead of the full sky in calculating the pulsar timing correlations [32]. Introducing a hemisphere into PTAs violates the spatial isotropy, such that hemisphere-averaged correlations can have a dependence on the DOA. However, there is a drawback in the hemisphere method, because the number of pulsars is reduced to nearly a half, resulting in a lower detection sensitivity.

Can there exist a method of estimating the DOA of GWs by using the whole of the observed pulsars? For tackling this problem, the main purpose of the present paper is to discuss correlations between quadrupole moments of pulsar timings over the full sky as well as over the whole observation time. We shall demonstrate that the DOA of the GW can be estimated in principle from the quadrupole-moment correlations.

This paper is organized as follows. Section 2 discusses quadrupole moments of the pulsar timings, where the correlations between the quadrupole moments are taken over the observed pulsar pairs as well as over the whole observation time. Section 3 studies a relationship among the correlations, a GW projection tensor, and a DOA estimation of GWs. Section 4 examines angular resolutions limited by the number of the pulsars as well as estimation errors by random noises. Section 5 is devoted to Summary. Appendix A provides a few steps for deriving Eq. (2.12), which plays a key role in this paper. Appendix B shows some relations between the GW polarization tensors, which are used in Section 3. Throughout this paper, the unit of  $c = 1$  is used and the center of the coordinates is chosen as the solar barycenter, safely approximated as the Earth.

## 2 Correlations of quadrupole tensors

### 2.1 Setup and notations

We suppose that  $N_p$  of pulsars are observed by a pulsar timing array. A pair of pulsars are labeled by  $a$  and  $b$  for  $a, b \in (1, 2, \dots, N_p)$ , where the directions of the  $a$ -th and  $b$ -th pulsars are denoted by unit vectors  $\hat{\Omega}_a$  and  $\hat{\Omega}_b$ , respectively.

The observed signals for the  $a$ -th and  $b$ -th pulsars are [5–8]

$$s_a(t) = z_a(t) + n_a(t), \quad (2.1)$$

$$s_b(t) = z_b(t) + n_b(t), \quad (2.2)$$

where  $z_a(t)$  and  $z_b(t)$  mean redshifts of a radio pulse due to GWs, and  $n_a(t)$  and  $n_b(t)$  are noises. We focus only on the Earth terms because pulsar terms vanish in the average e.g [4–6, 10, 33].

Let us imagine that a signal in a certain frequency bin of PTA observations is dominated by a distant SMBHB in circular motion and in the direction  $\hat{\Omega}_{GW}$  from the Earth. In the theory of general relativity, the redshifts are written as [5–8]

$$z_a(t) = h^+ F_a^+ \cos(\omega t) + h^\times F_a^\times \sin(\omega t), \quad (2.3)$$

$$z_b(t) = h^+ F_b^+ \cos(\omega t) + h^\times F_b^\times \sin(\omega t), \quad (2.4)$$

where  $h^+$  and  $h^\times$  denote constants for amplitudes of the plus and cross modes, respectively, and the initial phase of GWs can be zero by choosing an initial time. Here, the GW antenna patterns in the plane-wave approximation are defined as [5–8]

$$F_a^A \equiv \frac{1}{2} \frac{\hat{\Omega}_a^i \hat{\Omega}_a^j}{1 + \hat{\Omega}_{GW} \cdot \hat{\Omega}_a} e_{ij}^A(\hat{\Omega}_{GW}), \quad (2.5)$$

where  $e_{ij}^A(\hat{\Omega}_{GW})$  denotes the polarization tensor along the direction  $\hat{\Omega}_{GW}$  for  $A = +, \times$ . See References [34–38] for possible corrections by a nearby SMBHB and their cosmological implication. See also [40] for discussions on different frequencies emerging from the same

GW source in a search of new physics beyond general relativity. Beat effects can occur in the case that there are two SMBHBs that produce two GWs with very similar frequencies and comparable amplitudes at the Earth. A detection method for the beat effects has been discussed [41]. The present paper considers neither a gravity test nor a beat effect.

## 2.2 Correlations of quadrupole moments of pulsar timings

A quadrupole and traceless part of the redshifts over the sky can be defined as

$$I^{ij}(t) \equiv \frac{1}{4\pi} \oint d\Omega_a z_a(t) q_a^{ij}, \quad (2.6)$$

where  $\oint d\Omega_a$  is an integral over the full sky, and

$$q_a^{ij} \equiv \hat{\Omega}_a^i \hat{\Omega}_a^j - \frac{1}{3} \delta^{ij}. \quad (2.7)$$

The present paper employs the pulsar averaging [33].

A naive intuition may mislead to a candidate for correlations of quadrupole moments in pulsar timings as

$$\frac{1}{T_{obs}} \int_0^{T_{obs}} dt \left[ \left( \frac{1}{4\pi} \oint d\Omega_a (s_a(t) q_a^{ij}) \right) \left( \frac{1}{4\pi} \oint d\Omega_b (s_b(t+\tau) q_b^{ij}) \right) \right], \quad (2.8)$$

where the correlation among pulsar timings is taken over the full sky as well as the whole observation period  $T_{obs}$ , and  $\tau$  denotes a time lag in the autocorrelation. Here, the subscripts  $i$  and  $j$  are doubly written but not contracted with each other. As a result,  $q_a^{ij} q_b^{ij}$  is not a tensor but ill-defined in the simultaneous limit as  $\tau \rightarrow 0$ . Hence, the present paper does not employ the form of Eq. (2.8).

Therefore, we define another form as

$$Q^{ij} \equiv \frac{1}{T_{obs}} \int_0^{T_{obs}} dt \left[ \left( \frac{1}{4\pi} \oint d\Omega_a (s_a(t) q_a^{ik}) \right) \left( \frac{1}{4\pi} \oint d\Omega_b (s_b(t+\tau) q_b^{kj}) \right) \right], \quad (2.9)$$

where the summation is only for  $k$  as  $\sum_{k=1}^3$ . Note that  $q_a^{ik} q_b^{kj}$  is a tensor in the simultaneous limit as  $\tau \rightarrow 0$ .

We suppose that noises are random in space and time to follow

$$\begin{aligned} \oint d\Omega_a n_a(t) &= 0, \\ \oint d\Omega_a n_a(t) \hat{\Omega}_a &= 0, \\ \oint d\Omega_a n_a(t) q_a^{ij} &= 0, \\ \int_0^{T_{obs}} dt n_a(t) &= 0. \end{aligned} \quad (2.10)$$

The second and third equations in Eq. (2.10) mean that there are no dipole and quadrupole moments of noises. By using Eqs. (2.1), (2.2) and (2.10), Eq. (2.9) becomes

$$Q^{ij} = \frac{1}{T_{obs}} \int_0^{T_{obs}} dt \left[ \left( \frac{1}{4\pi} \oint d\Omega_a (z_a(t) q_a^{ik}) \right) \left( \frac{1}{4\pi} \oint d\Omega_b (z_b(t+\tau) q_b^{kj}) \right) \right], \quad (2.11)$$

The directional average of  $F_a^A q_a^{ij}$  for  $A = +, \times$  becomes

$$\frac{1}{4\pi} \oint d\Omega_a F_a^A q_a^{ij} = C_A e_A^{ij}(\hat{\Omega}_{GW}), \quad (2.12)$$

where the sum over  $A$  is not taken and  $C_A = 1/6$ . See Appendix A for a derivation of Eq. (2.12).

By using Eqs. (2.3), (2.4) and (2.12), Eq. (2.11) is calculated as

$$\begin{aligned} Q^{ij} = \frac{1}{36T_{obs}} \int_0^{T_{obs}} dt & \left( (h^+)^2 \cos(\omega t) \cos(\omega(t+\tau)) e_+^{ik}(\hat{\Omega}_{GW}) e_+^{kj}(\hat{\Omega}_{GW}) \right. \\ & + (h^\times)^2 \sin(\omega t) \sin(\omega(t+\tau)) e_\times^{ik}(\hat{\Omega}_{GW}) e_\times^{kj}(\hat{\Omega}_{GW}) \\ & + h^+ h^\times \left[ \cos(\omega t) \sin(\omega(t+\tau)) e_+^{ik}(\hat{\Omega}_{GW}) e_\times^{kj}(\hat{\Omega}_{GW}) \right. \\ & \left. \left. + \sin(\omega t) \cos(\omega(t+\tau)) e_\times^{ik}(\hat{\Omega}_{GW}) e_+^{kj}(\hat{\Omega}_{GW}) \right] \right). \quad (2.13) \end{aligned}$$

We use

$$\begin{aligned} e_+^{ik}(\hat{\Omega}_{GW}) e_+^{kj}(\hat{\Omega}_{GW}) &= P^{ij}, \\ e_\times^{ik}(\hat{\Omega}_{GW}) e_\times^{kj}(\hat{\Omega}_{GW}) &= P^{ij}, \\ e_+^{ik}(\hat{\Omega}_{GW}) e_\times^{kj}(\hat{\Omega}_{GW}) &= -\epsilon^{ijk} \hat{\Omega}_{GW}^k, \end{aligned} \quad (2.14)$$

where  $\epsilon^{ijk}$  is the Levi-Civita symbol, and the projection tensor with respect to  $\hat{\Omega}_{GW}$  is defined as [5, 6]

$$P^{ij} \equiv \delta^{ij} - \hat{\Omega}_{GW}^i \hat{\Omega}_{GW}^j. \quad (2.15)$$

See Appendix B for the derivation of Eq. (2.14).

Substituting Eq. (2.14) into Eq. (2.13) leads to

$$\begin{aligned} Q^{ij} = \frac{1}{36T_{obs}} \int_0^{T_{obs}} dt & \left( (h^+)^2 \cos(\omega t) \cos(\omega(t+\tau)) P^{ij} + (h^\times)^2 \sin(\omega t) \sin(\omega(t+\tau)) P^{ij} \right. \\ & \left. - h^+ h^\times \left[ \cos(\omega t) \sin(\omega(t+\tau)) - \sin(\omega t) \cos(\omega(t+\tau)) \right] \epsilon^{ijk} \hat{\Omega}_{GW}^k \right). \quad (2.16) \end{aligned}$$

Furthermore, we take the limit as  $T_{obs} \rightarrow \infty$ , which leads to  $\cos(\omega t) \cos(\omega(t+\tau)) \rightarrow \cos(\omega\tau)/2$ ,  $\sin(\omega t) \sin(\omega(t+\tau)) \rightarrow \cos(\omega\tau)/2$ ,  $\cos(\omega t) \sin(\omega(t+\tau)) \rightarrow \sin(\omega\tau)/2$ , and  $\sin(\omega t) \cos(\omega(t+\tau)) \rightarrow \sin(\omega\tau)/2$ . From Eq. (2.16), we thus arrive at

$$Q^{ij} \rightarrow \frac{1}{72} \left( \left[ (h^+)^2 + (h^\times)^2 \right] \cos(\omega\tau) P^{ij} - h^+ h^\times \sin(\omega\tau) \epsilon^{ijk} \hat{\Omega}_{GW}^k \right). \quad (2.17)$$

In addition, we suppose that the time lag is much shorter than the period of GWs (denoted as  $T_{GW}$ ), namely  $2\pi(\tau/T_{GW}) = \omega\tau \ll 1$ . As an example, we can imagine  $\tau = 2$  weeks, and  $T_{GW} = 12$  months. So, we take the limit as  $\omega\tau \rightarrow 0$ , which leads to  $\cos(\omega\tau) \rightarrow 1$  and  $\sin(\omega\tau) \rightarrow 0$ . Eq. (2.17) thus becomes

$$Q^{ij} \rightarrow KP^{ij}, \quad (2.18)$$

where

$$K \equiv \frac{1}{72}(h^{tot})^2, \quad (2.19)$$

and  $h^{tot} \equiv [(h^+)^2 + (h^\times)^2]^{1/2}$  is the GW intensity,

Some noise might contribute via the trace of  $Q^{ij}$ . In order to avoid such an error contamination from noises, it is convenient to consider the traceless part of  $Q^{ij}$ , which can be defined as

$$R^{ij} \equiv Q^{ij} - \frac{1}{3}Q\delta^{ij}, \quad (2.20)$$

where  $Q$  denotes the trace of  $Q^{ij}$ . From Eqs. (2.18) and (2.20),

$$\begin{aligned} R^{ij} &\rightarrow K \left( P^{ij} - \frac{1}{3}\delta^{ij}P^{kk} \right) \\ &= -Kq_{GW}^{ij}, \end{aligned} \quad (2.21)$$

where

$$q_{GW}^{ij} \equiv \hat{\Omega}_{GW}^i \hat{\Omega}_{GW}^j - \frac{1}{3}\delta^{ij}. \quad (2.22)$$

By calculating the traceless part of Eq. (2.9),  $R^{ij}$  is expressed in terms of the observed signals  $s_a(t)$  and  $s_b(t + \tau)$  as

$$R^{ij} = \frac{1}{(4\pi)^2 T_{obs}} \int_0^{T_{obs}} dt \oint d\Omega_a \oint d\Omega_b \left[ s_a(t)s_b(t + \tau) \left( q_a^{ik}q_b^{kj} - \frac{1}{3}[(\cos \gamma_{ab})^2 - \frac{1}{3}]\delta^{ij} \right) \right], \quad (2.23)$$

where  $\gamma_{ab}$  is a separation angle between the  $a$ -th and  $b$ -th pulsars, namely  $\cos \gamma_{ab} \equiv \hat{\Omega}_a \cdot \hat{\Omega}_b$ , and we use  $q_a^{ik}q_b^{ki} = (\cos \gamma_{ab})^2 - 1/3$ .

### 3 From quadrupole-moment correlations to DOA estimations

In this section, we shall discuss how to estimate  $\hat{\Omega}_{GW}$  from the matrix  $R^{ij}$ . From Eq. (2.21), we obtain  $\det(R) = -2K^3/27$ , where the determinant of  $R^{ij}$  is denoted as  $\det(R)$ , and  $\det(q_{GW}^{ij}) = 2/27$  is used. This equation is solved for  $K$  as

$$K = \left( -\frac{27 \det(R)}{2} \right)^{1/3}. \quad (3.1)$$

For  $i = x$  and  $j = x$ , Eq. (2.21) becomes  $R^{xx} = -K[(\hat{\Omega}_{GW}^x)^2 - 1/3]$ , which is solved for  $\hat{\Omega}_{GW}^x$  as

$$\hat{\Omega}_{GW}^x = \pm \sqrt{\frac{1}{3} - \frac{R^{xx}}{K}}. \quad (3.2)$$

There exist both signs of  $\pm$ , because  $P^{ij}$  does not distinguish  $\hat{\Omega}_{GW}$  from  $-\hat{\Omega}_{GW}$ .

For  $i = x$  and  $j = y$ , Eq. (2.21) reads  $R^{xy} = -K\hat{\Omega}_{GW}^x\hat{\Omega}_{GW}^y$ , which is rearranged as

$$\hat{\Omega}_{GW}^y = -\frac{R^{xy}}{K\hat{\Omega}_{GW}^x}, \quad (3.3)$$

where  $\hat{\Omega}_{GW}^x \neq 0$  is assumed. Similarly, Eq. (2.21) for  $i = z$  and  $j = x$  leads to

$$\hat{\Omega}_{GW}^z = -\frac{R^{zx}}{K\hat{\Omega}_{GW}^x}. \quad (3.4)$$

From PTA signals, we can estimate  $R^{ij}$ . The components of  $R^{ij}$  are substituted into Eqs. (3.2) - (3.4) to obtain the GW source direction  $\hat{\Omega}_{GW}$ .

For a unit vector  $\hat{\Omega}_{GW}$ , at least one of its components,  $\hat{\Omega}_{GW}^x$ ,  $\hat{\Omega}_{GW}^y$  and  $\hat{\Omega}_{GW}^z$  never vanishes. In a case of  $\hat{\Omega}_{GW}^x = 0$ , we should use counterparts of Eq. (3.2)-(3.4). If  $\hat{\Omega}_{GW}^y \neq 0$ ,

$$\hat{\Omega}_{GW}^y = \pm\sqrt{\frac{1}{3} - \frac{R^{yy}}{K}}. \quad (3.5)$$

$$\hat{\Omega}_{GW}^z = -\frac{R^{yz}}{K\hat{\Omega}_{GW}^y}, \quad (3.6)$$

$$\hat{\Omega}_{GW}^x = -\frac{R^{xy}}{K\hat{\Omega}_{GW}^y}. \quad (3.7)$$

If  $\hat{\Omega}_{GW}^z \neq 0$ ,

$$\hat{\Omega}_{GW}^z = \pm\sqrt{\frac{1}{3} - \frac{R^{zz}}{K}}. \quad (3.8)$$

$$\hat{\Omega}_{GW}^x = -\frac{R^{zx}}{K\hat{\Omega}_{GW}^z}, \quad (3.9)$$

$$\hat{\Omega}_{GW}^y = -\frac{R^{yz}}{K\hat{\Omega}_{GW}^z}. \quad (3.10)$$

Therefore, the present method can be used in principle for any DOA.

## 4 Discreteness, noises and estimation errors

### 4.1 From a continuous limit to a discrete distribution of pulsars

In this section, we take account that the number of the observed pulsars as well as that of the observations are finite. We suppose that a finite number ( $N_p$ ) of pulsars are observed for a whole observation time  $T_{obs}$  with a cadence  $P$ . Each of the pulsars is observed  $N_{obs} \equiv [T_{obs}/P] + 1$  times, where  $[ \ ]$  denotes a floor function.

Eq. (2.23) with Eq. (2.11) can be rewritten in terms of discrete sums as

$$R^{ij} = \frac{1}{\mathcal{K}_{max}(N_p)^2} \sum_{K=1}^{\mathcal{K}_{max}} \sum_{a=1}^{N_p} \sum_{b=1}^{N_p} \left[ s_a(t_K) s_b(t_K + \tau) \left( q_a^{ik} q_b^{kj} - \frac{1}{3} \left[ (\cos \gamma_{ab})^2 - \frac{1}{3} \right] \delta^{ij} \right) \right], \quad (4.1)$$

where  $K$  is a positive integer denoting the  $K$ -th observation,  $t_K \equiv P(K-1)$  denotes the  $K$ -th observation epoch, and  $\mathcal{K}_{max} \equiv [(T_{obs} - \tau + P)/P]$  means the number of the neighboring pair of  $t = t_K$  and  $t = t_K + \tau$  from  $t = 0$  to  $t = T_{obs}$ . In the rest of this paper, we adopt  $\tau = P$  for its simplicity. This leads to  $\mathcal{K}_{max} = N_{obs} - 1$ .

## 4.2 Angular resolution limited by the number of pulsars

Eq. (4.1) is a discretized version of Eq. (2.23) with Eq. (2.11). Let us imagine a random distribution of pulsars on the celestial sphere,  $\hat{\Omega}_a^i = \Omega_{aBG}^i + \delta_p \Omega_a^i$ , where  $\Omega_{aBG}^i$  corresponds to a homogeneous distribution, and the perturbation induced by a pulsar distribution is denoted by  $\delta_p$ . Namely,  $\Omega_{aBG}^i$  and  $\delta_p \Omega_a^i$  mean a background quantity and a perturbation, respectively. The random perturbation follows

$$\begin{aligned}
\frac{1}{N_p} \sum_{a=1}^{N_p} \delta_p \Omega_a^i &= 0, \\
\frac{1}{(N_p)^2} \sum_{a \neq b} \left( \delta_p \Omega_a^i \right) \left( \delta_p \Omega_b^j \right) &= 0, \\
\frac{1}{(N_p)^2} \sum_{a=1}^{N_p} \sum_{b=1}^{N_p} \left( \delta_p \Omega_a^i \right) \left( \delta_p \Omega_b^j \right) &= \frac{1}{(N_p)^2} \sum_{a=b} \left( \delta_p \Omega_a^i \right) \left( \delta_p \Omega_b^j \right) \\
&= \frac{1}{(N_p)^2} \sum_{a=1}^{N_p} \left( \delta_p \Omega_a^i \right) \left( \delta_p \Omega_a^j \right) \\
&= O\left(\frac{1}{N_p}\right), \tag{4.2}
\end{aligned}$$

where the second equation is used to show the first equality of the third equation, and  $|\delta_p \Omega_a^i| = O(1)$  is used in the last line. In a random distribution, the typical size of  $\delta_p \Omega_a^i$  is suppressed statistically by a factor  $O(1/\sqrt{N_p})$ .

From Eq. (4.1), a linear perturbation of  $R^{ij}$  induced by  $\delta_p \Omega_a^i$ , denoted as  $\delta_p R^{ij}$ , is expressed as

$$\delta_p R^{ij} = \frac{1}{\mathcal{K}_{max}(N_p)^2} \sum_{K=1}^{\mathcal{K}_{max}} \sum_{a=1}^{N_p} \sum_{b=1}^{N_p} \delta_p \left[ z_a(t_K) z_b(t_K + P) \left( q_a^{ik} q_b^{kj} - \frac{1}{3} \left[ (\cos \gamma_{ab})^2 - \frac{1}{3} \right] \delta^{ij} \right) \right]. \tag{4.3}$$

The fluctuation in the pulsar direction is not dependent on time during the PTA observation. Hence, the perturbation does not affect the time average procedure defined as  $(1/\mathcal{K}_{max}) \sum_K$  when we calculate the autocorrelation. Namely,  $(1/\mathcal{K}_{max}) \sum_K \sim O(1)$ . Hence, Eq. (4.3) becomes

$$\delta_p R^{ij} \sim \frac{1}{(N_p)^2} \sum_{a=1}^{N_p} \sum_{b=1}^{N_p} \delta_p \left[ z_a z_b \left( q_a^{ik} q_b^{kj} - \frac{1}{3} \left[ (\cos \gamma_{ab})^2 - \frac{1}{3} \right] \delta^{ij} \right) \right], \tag{4.4}$$

where  $z_a$  or  $z_b$  simply denote a typical value of  $z_a(t_K)$  or  $z_a(t_K + \tau)$ .

For the later convenience, first we obtain

$$\sum_{a=1}^{N_p} \sum_{b=1}^{N_p} z_a z_b \sim (N_p h^{tot})^2, \tag{4.5}$$

where we use  $z_a \sim z_b \sim O(h^{tot})$ .

The contribution of the  $\delta^{ij}$  term in Eq. (4.4) is a fraction  $\sim 5/6$ , because  $R^{ij}$  is a matrix with six independent components in the limit of  $\omega\tau \rightarrow 0$ . The factor  $\sim 5/6$  originating from the  $\delta^{ij}$  term is  $O(1)$  in the following order-of-magnitude estimation. Hence, we focus on the trace part of Eq. (4.4) as

$$\begin{aligned}\delta_p R^{ij} &\sim \frac{1}{(N_p)^2} \sum_{a=1}^{N_p} \sum_{b=1}^{N_p} \delta_p \left[ z_a z_b q_a^{ik} q_b^{kj} \right] \\ &\sim \frac{1}{(N_p)^2} \sum_{a=1}^{N_p} \sum_{b=1}^{N_p} z_a q_a^{ik} \delta_p(z_b q_b^{kj}).\end{aligned}\quad (4.6)$$

Note that the mean of  $\delta_p R^{ij}$  almost vanishes owing to the first equation of Eq. (4.2). By using Eq. (4.6), the variance of  $\delta_p R^{ij}$  is thus calculated as

$$(\delta_p R^{ij})^2 \sim \frac{1}{(N_p)^4} \sum_{a=1}^{N_p} \sum_{b=1}^{N_p} \sum_{c=1}^{N_p} \sum_{d=1}^{N_p} \left( z_a q_a^{ik} \delta_p(z_b q_b^{kj}) \right) \times \left( z_c q_c^{ik} \delta_p(z_d q_d^{kj}) \right), \quad (4.7)$$

where the summation is taken only for  $k$  but not for  $i, j$  (also in the rest of this subsection).

Next, we calculate

$$\begin{aligned}\sum_{a=1}^{N_p} \sum_{c=1}^{N_p} \left( z_a q_a^{ik} \times z_c q_c^{ik} \right) &\sim \sum_{a=1}^{N_p} \sum_{c=1}^{N_p} z_a z_c \\ &\sim O\left((N_p h^{tot})^2\right),\end{aligned}\quad (4.8)$$

where we use Eq. (4.5), and  $|q_a^{ik}| \sim |q_c^{ik}| \sim O(1)$ .

By using Eqs. (2.3), (2.4) and (2.5), we find  $\delta_p(z_b q_b^{ik}) \sim O(z_b q_b^{ik}) \times \delta_p \Omega_b^i \sim O(h^{tot}) \times O(\delta_p \Omega_b^i)$ , where  $O(z_a q_a^{ik}) \sim O(h^{tot})$  is used. By using  $\delta_p(z_b q_b^{ik}) \sim O(h^{tot}) \times O(\delta_p \Omega_b^i)$ , we thus obtain

$$\begin{aligned}&\sum_{b=1}^{N_p} \sum_{d=1}^{N_p} \left( \delta_p(z_b q_b^{kj}) \times \delta_p(z_d q_d^{kj}) \right) \\ &\sim O\left((h^{tot})^2\right) \times \sum_{b=1}^{N_p} \sum_{d=1}^{N_p} O\left(\delta_p \Omega_b^j \times \delta_p \Omega_d^j\right) \\ &\sim O\left(N_p (h^{tot})^2\right),\end{aligned}\quad (4.9)$$

where Eq. (4.2) is used in the last line.

By using Eqs. (4.8) and (4.9) in Eq. (4.7), we obtain

$$(\delta_p R^{ij})^2 \sim \frac{(h^{tot})^4}{N_p}, \quad (4.10)$$

where  $|q_a^{ij}| = O(1)$  is used. Therefore, the size of  $\delta_p R^{ij}$  is obtained as

$$|\delta_p R^{ij}| \sim \frac{(h^{tot})^2}{\sqrt{N_p}}. \quad (4.11)$$

We should note that  $h^{tot}$  cancels out from the ratio of  $R^{ij}/K$ , because  $R^{ij} \propto (h^{tot})^2$ , and  $K \propto (h^{tot})^2$ . By using Eq. (4.11), therefore, an accuracy in the components of the GW directional vector is

$$\begin{aligned} \left| \delta_p \hat{\Omega}_{GW}^i \right| &\sim \left| \frac{\delta_p R^{ij}}{K} \right| \\ &\sim O\left(\frac{1}{\sqrt{N_p}}\right), \end{aligned} \quad (4.12)$$

where Eqs. (3.2) - (3.10) are used in the first line. This leads to the angular resolution limited by the number of pulsars, which is obtained as

$$\begin{aligned} \left| \delta_p \hat{\Omega}_{GW} \right| &= \sqrt{\left| \delta_p \hat{\Omega}_{GW}^x \right|^2 + \left| \delta_p \hat{\Omega}_{GW}^y \right|^2 + \left| \delta_p \hat{\Omega}_{GW}^z \right|^2} \\ &\sim \sqrt{3} \times \sqrt{\left| \delta_p \hat{\Omega}_{GW}^i \right|^2} \\ &\sim \frac{\sqrt{3}}{\sqrt{N_p}}. \end{aligned} \quad (4.13)$$

Eq. (4.13) is the angular resolution limited by the number of pulsars in the present method. Roughly speaking, the angular resolution is  $\sim 0.2$  radian (corresponding to  $\sim 10$  degrees) for  $N_p \sim 100$  for instance.

### 4.3 Estimation error from a random noise

In this subsection, next, we shall discuss a typical size of the estimation error due to random noises, where we suppose  $n_a(t_K)$  and  $n_b(t_{K'})$  are white random noises with the zero mean and the common standard deviation  $\sigma$  for its simplicity. Let us write down relations between  $n_a(t_K)$  and  $n_b(t_{K'})$  for the later convenience. The zero mean for averaging over pulsar directions or over the whole observation time is expressed as

$$\frac{1}{N_p} \sum_{a=1}^{N_p} n_a(t_K) = 0, \quad (4.14)$$

$$\frac{1}{\mathcal{K}_{max}} \sum_{K=1}^{\mathcal{K}_{max}} n_a(t_K) = 0. \quad (4.15)$$

We assume that there are no correlations between different directions or between different observation epochs. They are written as

$$\frac{1}{(N_p)^2} \sum_{a \neq b} n_a(t_K) n_b(t_K) = 0, \quad (4.16)$$

$$\frac{1}{(\mathcal{K}_{max})^2} \sum_{K \neq K'} n_a(t_K) n_a(t_{K'}) = 0. \quad (4.17)$$

For its mathematical simplicity, we suppose the noises with the common variance  $\sigma^2$  as

$$\frac{1}{N_p} \sum_{a=1}^{N_p} (n_a(t_K))^2 = \sigma^2, \quad (4.18)$$

$$\frac{1}{\mathcal{K}_{max}} \sum_{K=1}^{\mathcal{K}_{max}} (n_a(t_K))^2 = \sigma^2. \quad (4.19)$$

For a correlation between noises observed at a simultaneous time, we find

$$\begin{aligned} \frac{1}{(N_p)^2} \sum_{a=1}^{N_p} \sum_{b=1}^{N_p} n_a(t_K) n_b(t_K) &= \frac{1}{(N_p)^2} \sum_{a=1}^{N_p} (n_a(t_K))^2 \\ &= \frac{\sigma^2}{N_p}, \end{aligned} \quad (4.20)$$

where Eqs. (4.16) and (4.18) are used in the first and second lines, respectively. Similarly, we find that noises for the same pulsar satisfy

$$\begin{aligned} \frac{1}{(\mathcal{K}_{max})^2} \sum_{K=1}^{\mathcal{K}_{max}} \sum_{K'=1}^{\mathcal{K}_{max}} n_a(t_K) n_a(t_{K'}) &= \frac{1}{(\mathcal{K}_{max})^2} \sum_{K=1}^{\mathcal{K}_{max}} (n_a(t_K))^2 \\ &= \frac{\sigma^2}{\mathcal{K}_{max}}, \end{aligned} \quad (4.21)$$

where Eqs. (4.17) and (4.19) are used in the first and second lines, respectively.

Let us discuss the perturbation of  $R^{ij}$  owing to the noises, denoted as  $\delta_n R^{ij}$ , which is roughly

$$\delta_n R^{ij} \sim \left( \frac{1}{\mathcal{K}_{max} (N_p)^2} \sum_{K=1}^{\mathcal{K}_{max}} \sum_{a=1}^{N_p} \sum_{b=1}^{N_p} n_a(t_K) n_b(t_K + P) \right). \quad (4.22)$$

Here, we focus on the quadratic terms in noises in Eq. (4.1) by ignoring the coupling terms of GWs and noises, because the coupling terms are  $\sim h^{tot} \times \sigma$ , the quadratic noise terms are  $\sigma^2$ , and  $h^{tot} \ll \sigma$  is expected for the current PTA observations.

Note that the mean of  $\delta_n R^{ij}$  vanishes owing to Eq. (4.15). Therefore, the variance of

$R^{ij}$  is thus calculated as

$$\begin{aligned}
& (\delta_n R^{ij})^2 \\
& \sim \left( \frac{1}{\mathcal{K}_{max}(N_p)^2} \sum_{K=1}^{\mathcal{K}_{max}} \sum_{a=1}^{N_p} \sum_{b=1}^{N_p} n_a(t_K) n_b(t_K + P) \right) \\
& \quad \times \left( \frac{1}{\mathcal{K}_{max}(N_p)^2} \sum_{K'=1}^{\mathcal{K}_{max}} \sum_{c=1}^{N_p} \sum_{d=1}^{N_p} n_c(t_{K'}) n_d(t_{K'} + P) \right) \\
& \sim \frac{1}{(\mathcal{K}_{max})^2 (N_p)^4} \sum_{K=1}^{\mathcal{K}_{max}} \left( \sum_{a=1}^{N_p} \sum_{c=1}^{N_p} n_a(t_K) n_c(t_K) \right) \\
& \quad \times \left( \sum_{b=1}^{N_p} \sum_{d=1}^{N_p} n_b(t_K + P) n_d(t_K + P) \right) \\
& \sim \frac{1}{(\mathcal{K}_{max})^2 (N_p)^4} \times \sum_{K=1}^{\mathcal{K}_{max}} (N_p \times \sigma^2)^2 \\
& \sim \frac{\sigma^4}{\mathcal{K}_{max}(N_p)^2}, \tag{4.23}
\end{aligned}$$

where Eqs. (4.15) and (4.17) are used in the fourth and fifth lines, respectively, and Eq. (4.18) is used in the sixth line. Note that the summation is not taken for  $i, j$

By using Eq. (4.23), the size of  $\delta_n R^{ij}$  is obtained as

$$\begin{aligned}
|\delta_n R^{ij}| &= \sqrt{(\delta_n R^{ij})^2} \\
&\sim \frac{\sigma^2}{N_p \sqrt{N_{obs}}}, \tag{4.24}
\end{aligned}$$

where we use  $\mathcal{K}_{max} \approx N_{obs}$  for  $N_{obs} \gg 1$ .

The ratio of  $\delta_n R^{ij}$  to  $R^{ij}$  gives us a typical size of the estimation error for a component of the GW directional vector. It is

$$\begin{aligned}
|\delta_n \hat{\Omega}_{GW}^i| &\sim \left| \frac{\delta_n R^{ij}}{R_{GW}^{ij}} \right| \\
&\sim \frac{1}{N_p \sqrt{N_{obs}}} \times \left( \frac{\sigma}{h^{tot}} \right)^2, \tag{4.25}
\end{aligned}$$

where  $R_{GW}^{ij}$  denotes the purely GW part of  $R^{ij}$ , and we use  $R_{GW}^{ij} \sim (h^{tot})^2$  from Eqs. (2.19) and (2.21). This leads to the typical size of an estimation error in the GW direction as

$$\begin{aligned}
|\delta_n \hat{\Omega}_{GW}| &= \sqrt{|\delta_n \hat{\Omega}_{GW}^x|^2 + |\delta_n \hat{\Omega}_{GW}^y|^2 + |\delta_n \hat{\Omega}_{GW}^z|^2} \\
&\sim \sqrt{3} \times \sqrt{|\delta_n \hat{\Omega}_{GW}^i|^2} \\
&\sim \frac{\sqrt{3}}{N_p \sqrt{N_{obs}}} \times \left( \frac{\sigma}{h^{tot}} \right)^2, \tag{4.26}
\end{aligned}$$

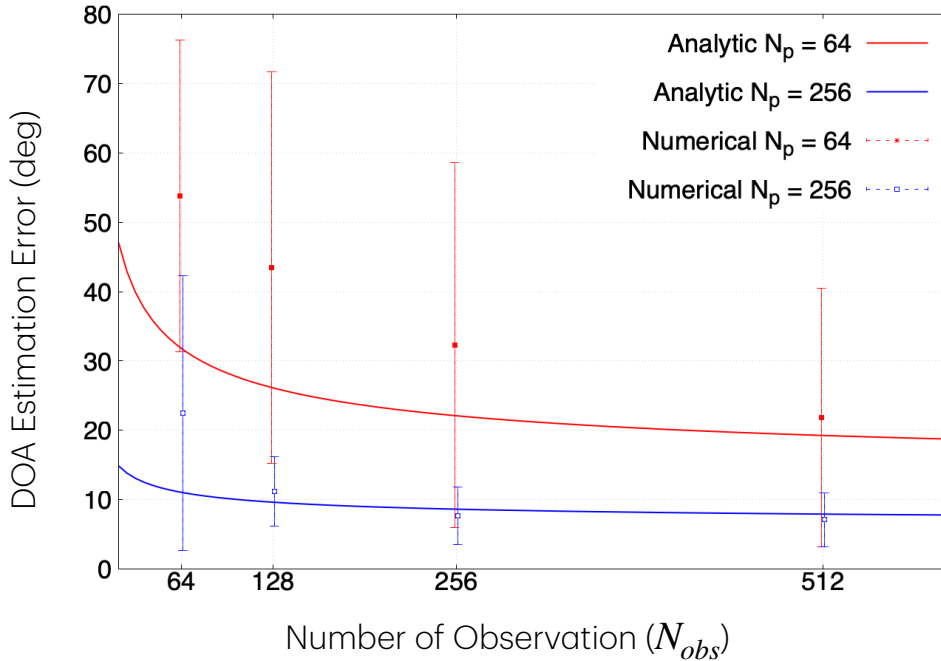


**Figure 1.** DOA estimation errors limited by the numbers of observed pulsars and observation epochs. The vertical axis denotes the DOA estimation error for the GW, while the horizontal axis means the number of observation epochs  $N_{obs}$ . The solid (red in color) and dashed (blue in color) curves are theoretical curves for  $N_p = 64$  and  $N_p = 256$ , respectively, where  $h^+ = h^\times = 1$  and  $\sigma = 10$  are chosen, and the DOA estimation error is estimated as a sum of  $\delta_p \hat{\Omega}_{GW}$  and  $\delta_n \hat{\Omega}_{GW}$  in Eqs. (4.13) and (4.26), respectively. The filled (red in color) and empty (blue in color) squares denote the mean of the error for for  $N_p = 64$  and  $N_p = 256$ , respectively, and the error bar corresponds to one sigma error, where 100 runs are numerically performed.

This is evaluated as

$$\left| \delta_n \hat{\Omega}_{GW} \right| \sim 0.1 \left( \frac{128}{N_p} \right) \left( \frac{24}{N_{obs}} \right)^{1/2} \left( \frac{\sigma}{10} \right)^2 \left( \frac{\sqrt{2}}{h^{tot}} \right)^2. \quad (4.27)$$

Roughly speaking, the estimation error is  $\sim 0.1$  radian (corresponding to  $\sim 6$  degrees) for e.g.  $N_p \sim 100$ ,  $N_{obs} \sim 24$ ,  $\sigma/h^+ \sim \sigma/h^\times \sim 10$ .

Figure 1 shows numerical plots for estimation errors of the DOA by using the present method. Figure 2 shows a scatter of estimated DOAs for  $N_p = 256$  and  $N_{obs} = 256$  (e.g.  $\tau \sim 2$  weeks and  $T_{obs} \sim 10$  years), where  $h^+ = h^\times = 1$  and  $\sigma = 10$  are chosen and 100 runs are performed. The two panels in Figure 2 correspond to a plot for  $N_p = 256$  and  $N_{obs} = 256$  in Figure 1. Theoretical estimations of Eqs. (4.13) and (4.26) are consistent with the numerical results in Figures 1 and 2.

In the left panel of Figure 2, several dots are located at points completely different from the true DOA (denoted by a red disk). This suggests that  $N_p = 64$  (roughly corresponding to the current status of PTAs [11–14]) is not enough to precisely estimate DOAs by using the quadrupole-correlation method. Drawing a definite conclusion needs more detailed investigations based on a more realistic noise model for a realistic pulsar distribution.

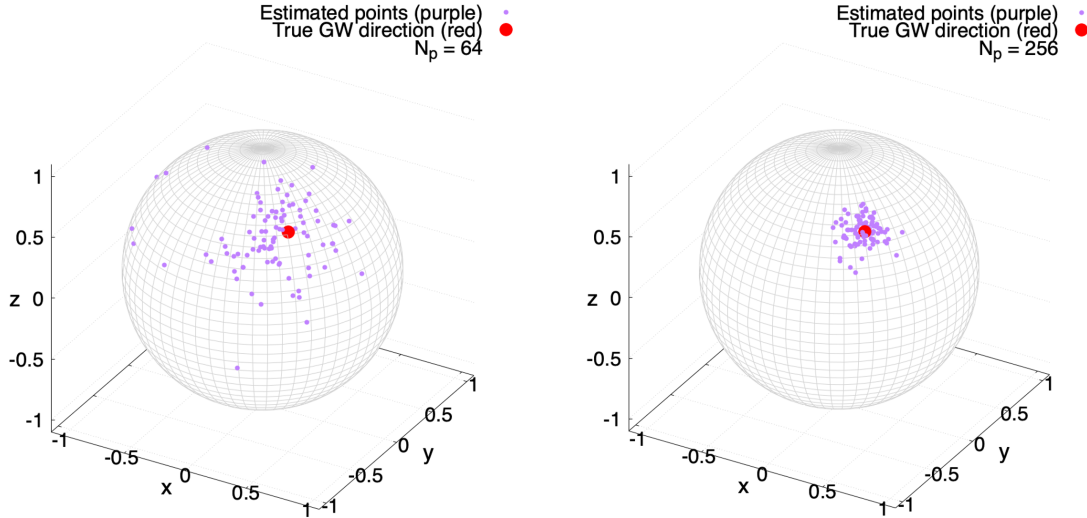


**Figure 2.** Scatter plots of DOA estimations for a single GW.  $h^+ = h^\times = 1$ , and  $\sigma = 10$  are chosen for  $N_{obs} = 256$ , and 100 runs are numerically performed. Here,  $\hat{\Omega}_{GW} = (x, y, z)$  is chosen as  $\theta_{GW} = \phi_{GW} = 45$  deg. Two panels (left:  $N_p = 64$ , right:  $N_p = 256$ ) correspond to two squares in Figure 1, where one filled square in Figure 1 is for  $N_p = 64$  and  $N_{obs} = 256$ , and the other empty square in the same figure is for  $N_p = 256$  and  $N_{obs} = 256$ .

The left panel of Figure 2 for  $N_p = 256$ , on the other hand, demonstrates that the present method will potentially allow a DOA estimation. The latter case encourages us to await SKA that will find hundreds of pulsars.

#### 4.4 Single dominant source over an isotropic stochastic background

Finally, let us mention a possible way to make the scenario more realistic. We suppose a single SMBHB that dominates over a stochastic background in a certain frequency bin of PTA observations, where the signal can be expressed as  $s_a(t) = z_a(t) + z_{aBG}(t) + n_a(t)$  for  $z_{aBG}$  denoting the redshift due to the stochastic background.

For its simplicity, we assume the isotropic stochastic background possibly generated by inflation, for which there is no quadrupole moment of the redshifts due to the background GW, namely  $\oint d\Omega_a z_{aBG}(t) q_a^{ij} = 0$ . From Eq. (2.9), we can thus arrive at Eq. (2.18). Therefore, the present formulation and method stand also in this situation.

## 5 Summary

We discussed correlations between the quadrupole moments of pulsar timings due to GWs, where we supposed that an isolated source such as a SMBHB dominates over the isotropic

stochastic background in a certain bin of the PTA frequency domain. This situation was formulated to demonstrate that a DOA of a GW can be estimated in principle. The angular resolution as well as estimation error in the present method was studied. According to the analytical and numerical calculations, the forthcoming SKA will make the DOA estimation possible.

Is the present method applicable also in the presence of a sub-dominant GW component in the same frequency bin? Do higher multipole moments such as octupole moments play any role in improving the DOA estimation? These issues are left for future.

## A Derivation of Eq. (2.12) with $C_A$

In this appendix, we shall derive Eq. (2.12) by several steps as follows.

Let us begin with the angular average of PTA antenna pattern functions in Eq. (2.5), which is defined as

$$\frac{1}{4\pi} \oint d\Omega_a F_a^A = \frac{1}{8\pi} e_{ij}^A(\hat{\Omega}_{GW}) \oint d\Omega_a \frac{\hat{\Omega}_a^i \hat{\Omega}_a^j}{1 + \hat{\Omega}_{GW} \cdot \hat{\Omega}_a}. \quad (\text{A.1})$$

The integral in the right-hand side of Eq. (A.1) is symmetric between  $i$  and  $j$ , while the integrand depends on  $\hat{\Omega}_{GW}$ . Therefore, the integral is a linear combination of  $\delta^{ij}$  and  $\hat{\Omega}_{GW}^i \hat{\Omega}_{GW}^j$ . Therefore,

$$\frac{1}{4\pi} \oint d\Omega_a F_a^A = 0, \quad (\text{A.2})$$

where we use the transverse and traceless property as  $e_{ij}^A(\hat{\Omega}_{GW}) \hat{\Omega}_{GW}^i \hat{\Omega}_{GW}^j = 0$  and  $e_{ij}^A(\hat{\Omega}_{GW}) \delta^{ij} = 0$ .

Secondly, we consider the angular average of a dipole part of the antenna pattern, defined as

$$\frac{1}{4\pi} \oint d\Omega_a F_a^A \hat{\Omega}_a^k = \frac{1}{8\pi} e_{ij}^A(\hat{\Omega}_{GW}) \oint d\Omega_a \frac{\hat{\Omega}_a^i \hat{\Omega}_a^j \hat{\Omega}_a^k}{1 + \hat{\Omega}_{GW} \cdot \hat{\Omega}_a}. \quad (\text{A.3})$$

The integral in the right-hand side of Eq. (A.3) is totally symmetric among  $i, j, k$ , and it depends on  $\hat{\Omega}_{GW}$ . Hence, the integral is proportional  $\delta^{ij} \hat{\Omega}_{GW}^k + \delta^{jk} \hat{\Omega}_{GW}^i + \delta^{ki} \hat{\Omega}_{GW}^j$ . Therefore,

$$\frac{1}{4\pi} \oint d\Omega_a F_a^A \hat{\Omega}_a^k = 0, \quad (\text{A.4})$$

where we use  $e_{ik}^A(\hat{\Omega}_{GW}) \hat{\Omega}_{GW}^k = 0$  and  $e_{ij}^A(\hat{\Omega}_{GW}) \delta^{ij} = 0$ .

Thirdly, we examine the angular average of a quadrupole part of the antenna pattern, defined as

$$\frac{1}{4\pi} \oint d\Omega_a F_a^A \hat{\Omega}_a^k \hat{\Omega}_a^l = \frac{1}{8\pi} e_{ij}^A(\hat{\Omega}_{GW}) \oint d\Omega_a \frac{\hat{\Omega}_a^i \hat{\Omega}_a^j \hat{\Omega}_a^k \hat{\Omega}_a^l}{1 + \hat{\Omega}_{GW} \cdot \hat{\Omega}_a}. \quad (\text{A.5})$$

The integral in the right-hand side of Eq. (A.5) is totally symmetric among  $i, j, k, l$ , and it depends on  $\hat{\Omega}_{GW}$ . Therefore, the integral is written as a linear combination of three types as  $\delta^{ij} \delta^{kl}$  (and its permutations),  $\delta^{ij} \hat{\Omega}_{GW}^k \hat{\Omega}_{GW}^l$  (and its permutations), and  $\hat{\Omega}_{GW}^i \hat{\Omega}_{GW}^j \hat{\Omega}_{GW}^k \hat{\Omega}_{GW}^l$ .

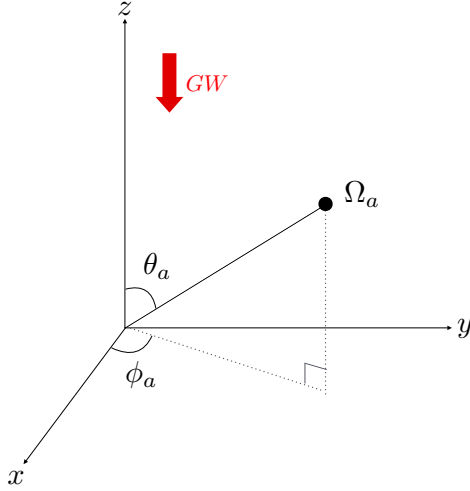


**Figure 3.** The polar coordinates associated with Eq. (A.7) and  $\hat{\Omega}_{GW} = (0, 0, 1)$ .

Most of them vanish for  $e_{ij}^A(\hat{\Omega}_{GW})$ , because they are longitude or a trace part. Only the nonvanishing terms are  $(\delta^{ik}\delta^{jl} + \delta^{il}\delta^{jk})e_{ij}^A(\hat{\Omega}_{GW}) = 2e_{kl}^A(\hat{\Omega}_{GW})$ . Therefore, we find

$$\frac{1}{4\pi} \oint d\Omega_a F_a^A \hat{\Omega}_a^k \hat{\Omega}_a^l = C_A e_{kl}^A(\hat{\Omega}_{GW}), \quad (\text{A.6})$$

where  $C_A$  is a certain constant to be calculated below.

We choose Cartesian coordinates satisfying

$$e_{ij}^A(\hat{\Omega}_{GW}) = \begin{pmatrix} 1 & 0 & 0 \\ 0 & -1 & 0 \\ 0 & 0 & 0 \end{pmatrix}, \quad (\text{A.7})$$

where we assume  $\hat{\Omega}_{GW} = (0, 0, 1)$ . See Figure 3 for a schematic figure of  $\hat{\Omega}_{GW}$  in the adopted coordinates. Note that it is possible to choose  $\hat{\Omega}_{GW} = (0, 0, -1)$ , because a forward direction or a backward one does not matter in this appendix.

For  $k = x$  and  $l = x$ , Eq. (A.6) becomes

$$\frac{1}{4\pi} \oint d\Omega_a F_a^A (\hat{\Omega}_a^x)^2 = C_+, \quad (\text{A.8})$$

where Eq. (A.7) is used.  $\hat{\Omega}_a = (\sin \theta_a \cos \phi_a, \sin \theta_a \sin \phi_a, \cos \theta_a)$  in the polar coordinates is substituted into the left-hand side of Eq. (A.8). Straightforward calculations of the left-hand side in Eq. (A.8) lead to

$$\frac{1}{4\pi} \oint d\Omega_a \frac{\sin \theta_a \cos(2\phi_a) (\sin \theta_a \cos \phi_a)^2}{1 + \cos \theta_a} = \frac{1}{6}. \quad (\text{A.9})$$

Therefore,  $C_+ = 1/6$ . Similarly, we obtain  $C_\times = 1/6$ . As a result,  $C_A = 1/6$  for any of  $A = +, \times$ .

It follows that the trace part of Eq. (A.6) leads to Eq. (A.2), because  $\hat{\Omega}_a$  is a unit vector. Hence, the traceless part of Eq. (A.6) becomes Eq. (2.12), because  $q_{ab}^{kl}$  is the traceless part of  $\hat{\Omega}_a^k \hat{\Omega}_a^l$  and  $e_{kl}^A(\hat{\Omega}_{GW})$  is traceless.

An alternative and straightforward method for deriving Eq. (2.12) is to adopt the coordinates associated with Eq. (A.7) when we calculate  $C_A$ . Then, the left-hand side of Eq. (2.12) for  $A = +$  is directly calculated as  $1/6$  ( $k = x, l = x$ ),  $-1/6$  ( $k = y, l = y$ ), and  $0$  (otherwise), while that for  $A = \times$  is  $1/6$  ( $k = x, l = y$  and  $k = y, l = x$ ) and  $0$  (otherwise). Expressions for these results lead to Eq. (2.12) again.

## B Relationship between quadratic polarization tensors

We adopt the spatial orthonormal vectors  $\hat{l}, \hat{m}, \hat{n}$  in the right-handed system, where  $\hat{l}$  denotes the direction of GW propagation. The polarization tensors  $e_{ij}^A(\hat{\Omega}_{GW})$  can be written as [5–8]

$$e_{ij}^+(\hat{\Omega}_{GW}) = \hat{m}_i \hat{m}_j - \hat{n}_i \hat{n}_j, \quad (\text{B.1})$$

$$e_{ij}^\times(\hat{\Omega}_{GW}) = \hat{m}_i \hat{n}_j + \hat{n}_i \hat{m}_j. \quad (\text{B.2})$$

Note that the GW source direction is opposite to the propagation direction, namely  $\hat{\Omega}_{GW} = -\hat{l}$ . Therefore,  $\hat{m}, \hat{n}, \hat{\Omega}_{GW}$  are in the left-handed system.

From Eq. (B.1), we find

$$\begin{aligned} e_{ik}^+(\hat{\Omega}_{GW})e_{kj}^+(\hat{\Omega}_{GW}) &= (\hat{m}_i \hat{m}_k - \hat{n}_i \hat{n}_k)(\hat{m}_k \hat{m}_j - \hat{n}_k \hat{n}_j) \\ &= \hat{m}_i \hat{m}_j + \hat{n}_i \hat{n}_j \\ &= \delta_{ij} - \hat{\Omega}_{GW}^i \hat{\Omega}_{GW}^j, \end{aligned} \quad (\text{B.3})$$

where  $\delta_{ij} = \hat{m}_i \hat{m}_j + \hat{n}_i \hat{n}_j + \hat{\Omega}_{GW}^i \hat{\Omega}_{GW}^j$  is used in the last line. By using Eq. (2.15), we obtain

$$e_{ik}^+(\hat{\Omega}_{GW})e_{kj}^+(\hat{\Omega}_{GW}) = P_{ij}. \quad (\text{B.4})$$

From Eq. (B.2), we obtain

$$\begin{aligned} e_{ik}^\times(\hat{\Omega}_{GW})e_{kj}^\times(\hat{\Omega}_{GW}) &= (\hat{m}_i \hat{n}_k + \hat{n}_i \hat{m}_k)(\hat{m}_k \hat{n}_j + \hat{n}_k \hat{m}_j) \\ &= \hat{m}_i \hat{m}_j + \hat{n}_i \hat{n}_j \\ &= \delta_{ij} - \hat{\Omega}_{GW}^i \hat{\Omega}_{GW}^j, \end{aligned} \quad (\text{B.5})$$

where  $\delta_{ij} = \hat{m}_i \hat{m}_j + \hat{n}_i \hat{n}_j + \hat{\Omega}_{GW}^i \hat{\Omega}_{GW}^j$  is used in the last line. By using Eq. (2.15), we obtain

$$e_{ik}^\times(\hat{\Omega}_{GW})e_{kj}^\times(\hat{\Omega}_{GW}) = P_{ij}. \quad (\text{B.6})$$

From Eqs. (B.1) and (B.2), we compute

$$\begin{aligned} e_{ik}^+(\hat{\Omega}_{GW})e_{kj}^\times(\hat{\Omega}_{GW}) &= (\hat{m}_i \hat{m}_k - \hat{n}_i \hat{n}_k)(\hat{m}_k \hat{n}_j + \hat{n}_k \hat{m}_j) \\ &= \hat{m}_i \hat{n}_j - \hat{n}_i \hat{m}_j. \end{aligned} \quad (\text{B.7})$$

In the left-handed system,  $\hat{\Omega}_{GW} = -\hat{l} = -(\hat{m} \times \hat{n})$ , which is rewritten as  $\hat{\Omega}_{GW}^i = -\epsilon^{ijk} \hat{m}_j \hat{n}_k$ . This leads to  $\epsilon^{ijk} \hat{\Omega}_{GW}^k = \hat{m}_i \hat{n}_j - \hat{n}_i \hat{m}_j$ . By using this for the last line in Eq. (B.7), we arrive at

$$e_{ik}^+(\hat{\Omega}_{GW})e_{kj}^\times(\hat{\Omega}_{GW}) = -\epsilon^{ijk} \hat{\Omega}_{GW}^k. \quad (\text{B.8})$$

## Acknowledgments

We are grateful to Shun Yamamoto, Keitaro Takahashi, Mariko Nomura, and Yuuiti Sendouda for useful discussions. We wish to thank JGRG34 workshop participants for stimulating conversations. This work was supported in part by Japan Society for the Promotion of Science (JSPS) Grant-in-Aid for Scientific Research, No. 24K07009(H.A.).

## References

- [1] F. B. Estabrook, and H. D. Wahlquist, "Response of Doppler spacecraft tracking to gravitational radiation," *General Relativ. Grav.*, **6**, 439 (1975).
- [2] M. V. Sazhin, "Opportunities for detecting ultralong gravitational waves," *Soviet Ast.*, **22**, 36 (1978).
- [3] S. Detweiler, "Pulsar timing measurements and the search for gravitational waves," *Astrophys. J.* **234**, 1100 (1979).
- [4] R. W. Hellings, and G. S. Downs, "Upper limits on the isotropic gravitational radiation background from pulsar timing analysis," *Astrophys. J. Lett.*, **265**, L39 (1983).
- [5] J. D. E. Creighton, and W. G. Anderson, *Gravitational-Wave Physics and Astronomy: An Introduction to Theory, Experiment and Data Analysis* (Wiley, NY 2013).
- [6] M. Maggiore, *Gravitational Waves: Astrophysics and Cosmology* (Oxford Univ. Press, UK, 2018).
- [7] M. Anholm, S. Ballmer, J. D. E. Creighton, L. R. Price, and X. Siemens, "Optimal strategies for gravitational wave stochastic background searches in pulsar timing data," *Phys. Rev. D* **79**, 084030 (2009).
- [8] F. A. Jenet, and J. D. Romano, "Understanding the gravitational-wave Hellings and Downs curve for pulsar timing arrays in terms of sound and electromagnetic waves," *Am. J. Phys.* **83**, 635 (2015).
- [9] J. D. Romano, and N. J. Cornish, "Detection methods for stochastic gravitational-wave backgrounds: a unified treatment," *Living Rev. Relativ.* **20**, 2 (2017).
- [10] J. D. Romano, and B. Allen, "Answers to frequently asked questions about the pulsar timing array Hellings and Downs curve," *Class. Quantum Grav.* **41**, 175008 (2024).
- [11] G. Agazie, et al., "The NANOGrav 15 yr Data Set: Evidence for a Gravitational-wave Background," *Astrophys. J. Lett.* **951**, L8 (2023).
- [12] J. Antoniadis, et al., "The second data release from the European Pulsar Timing Array," *Astron. Astrophys.* **678**, A50 (2023).
- [13] D. J. Reardon, et al., "Search for an Isotropic Gravitational-wave Background with the Parkes Pulsar Timing Array," *Astrophys. J. Lett.* **951**, L6 (2023).
- [14] H. Xu, et al., "Searching for the Nano-Hertz Stochastic Gravitational Wave Background with the Chinese Pulsar Timing Array Data Release I," *Res. Astron. Astrophys.* **23**, 075024 (2023).
- [15] Z. Chen, C. Yuan, and Q. Huang, "Pulsar Timing Array Constraints on Primordial Black Holes with NANOGrav 11-Year Dataset," *Phys. Rev. Lett.* **124**, 251101 (2020).
- [16] J. Ellis, and M. Lewicki, "Cosmic String Interpretation of NANOGrav Pulsar Timing Data," *Phys. Rev. Lett.* **126**, 041304 (2021).
- [17] C. Smarra et al. (European Pulsar Timing Array), "Second Data Release from the European Pulsar Timing Array: Challenging the Ultralight Dark Matter Paradigm," *Phys. Rev. Lett.* **131**, 171001 (2023).

- [18] Y. Gouttenoire, "First-Order Phase Transition Interpretation of Pulsar Timing Array Signal Is Consistent with Solar-Mass Black Holes," *Phys. Rev. Lett.* **131**, 171404 (2023).
- [19] G. Franciolini, A. J. Iovino, V. Vaskonen, and H. Veermae, "Recent Gravitational Wave Observation by Pulsar Timing Arrays and Primordial Black Holes: The Importance of Non-Gaussianities," *Phys. Rev. Lett.* **131**, 201401 (2023).
- [20] G. Franciolini, D. Racco, and F. Rompineve, "Footprints of the QCD Crossover on Cosmological Gravitational Waves at Pulsar Timing Arrays," *Phys. Rev. Lett.* **132**, 081001 (2024).
- [21] W. DeRocco, and J. A. Dror, "Using Pulsar Parameter Drifts to Detect Subnanohertz Gravitational Waves," *Phys. Rev. Lett.* **132**, 101403 (2024).
- [22] D. G. Figueroa, M. Pieroni, A. Ricciardone, and P. Simakachorn, "Cosmological Background Interpretation of Pulsar Timing Array Data," *Phys. Rev. Lett.* **132**, 171002 (2024).
- [23] P. Athron, A. Fowlie, C. Lu, L. Morris, L. Wu, Y. Wu, and Z. Xu, "Can Supercooled Phase Transitions Explain the Gravitational Wave Background Observed by Pulsar Timing Arrays?," *Phys. Rev. Lett.* **132**, 221001 (2024).
- [24] D. Shih, M. Freytsis, S. R. Taylor, J. A. Dror, and N. Smyth, "Fast Parameter Inference on Pulsar Timing Arrays with Normalizing Flows," *Phys. Rev. Lett.* **133**, 011402 (2024).
- [25] N. A. Kumar, and M. Kamionkowski, "Efficient Computation of Overlap Reduction Functions for Pulsar Timing Arrays," *Phys. Rev. Lett.* **133**, 151401 (2024).
- [26] L. Bian, S. Ge, J. Shu, B. Wang, X. Yang, and J. Zong, "Gravitational wave sources for pulsar timing arrays," *Phys. Rev. D* **109**, L101301 (2024).
- [27] Z. Chen, J. Li, L. Liu, and Z. Yi, "Probing the speed of scalar-induced gravitational waves with pulsar timing arrays," *Phys. Rev. D* **109**, L101302 (2024).
- [28] B. Allen, "Variance of the Hellings-Downs correlation," *Phys. Rev. D* **107**, 043018 (2023).
- [29] B. Allen, "Pulsar timing array harmonic analysis and source angular correlations," *Phys. Rev. D* **110**, 043043 (2024).
- [30] L. S. Finn, and A. N. Lommen, "Detection, Localization and Characterization of Gravitational Wave Bursts in a Pulsar Timing Array," *Astrophys. J.* **718**, 1400 (2010).
- [31] B. J. Burt, A. N. Lommen, and L. S. Finn, "Optimizing Pulsar Timing Arrays to Maximize Gravitational Wave Single Source Detection: a First Cut," *Astrophys. J.* **730**, 17 (2011).
- [32] T. Sasaki, K. Yamauchi, S. Yamamoto, and H. Asada, "Hemisphere-averaged Hellings-Downs curve between pulsar pairs for a gravitational wave source," *Phys. Rev. D* **109**, 024023 (2024).
- [33] N. J. Cornish, and A. Sesana, "Pulsar timing array analysis for black hole backgrounds," *Class. Quantum Grav.* **30**, 224005 (2013).
- [34] C. McGrath, and J. Creighton, "Fresnel models for gravitational wave effects on pulsar timing," *Mon. Not. Roy. Soc. Astron.* **505**, 4531 (2021).
- [35] C. McGrath, D. J. D'Orazio, and J. Creighton, "Measuring the Hubble constant with double gravitational wave sources in pulsar timing," *Mon. Not. Roy. Soc. Astron.* **517**, 1242 (2022).
- [36] X. Guo, Y. Lu, and Q. Yu, "On Detecting Nearby Nanohertz Gravitational Wave Sources via Pulsar Timing Arrays," *Astrophys. J.* **939**, 55 (2022).
- [37] R. Kubo, K. Yamahira, and H. Asada, "Pulsar Timing Response to Gravitational Waves with Spherical Wavefronts from a Massive Compact Source in the Quadrupole Approximation," *Astrophys. J.* **946**, 76 (2023).
- [38] D. J. D'Orazio, and A. Loeb, "Using Gravitational Wave Parallax to Measure the Hubble Parameter with Pulsar Timing Arrays," *Phys. Rev. D* **104**, 063015 (2021).

- [39] E. Poisson, and C. M. Will, *Gravity*, (Cambridge Univ. Press, UK. 2014).
- [40] W. Hu, Q. Liang, M. Lin, and M. Trodden, JCAP **12**, 054 (2024).
- [41] S. Yamamoto, and H. Asada, JCAP **10**, 058 (2025).